JACC Vol. 28, No. 5
November 1, 1996:1134–9

Chronic Arterial Responses to Stent Implantation: A Serial Intravascular Ultrasound Analysis of Palmaz-Schatz Stents in Native Coronary Arteries

RAINER HOFFMANN, MD, GARY S. MINTZ, MD, FACC, JEFFREY J. POPMA, MD, FACC, LOWELL F. SATLER, MD, FACC, AUGUSTO D. PICHARD, MD, FACC, KENNETH M. KENT, MD, PHD, FACC, CAROL WALSH, PAUL MACKELL, MARTIN B. LEON, MD, FACC

Washington, D.C.

Objectives. **We used intravascular ultrasound (IVUS) imaging to evaluate the chronic vessel responses to Palmaz-Schatz stents.**

Background. **Palmaz-Schatz stents have been shown to inhibit early elastic recoil and late arterial remodeling while triggering neointimal hyperplasia. However, changes occurring in native vessels surrounding stent struts have not been well studied.**

Methods. **Postintervention and follow-up (mean [±SD] 5.4 ± 3.8 months) serial IVUS imaging was performed in 25 stents without restenosis and 24 with in-stent restenosis. Intravascular ultrasound imaging using automatic transducer pullback at 0.5 mm/s allowed measurement at 1-mm axial increments of external elastic membrane (EEM), stent and lumen cross-sectional areas (CSAs) and calculation of peristent plaque plus media (P+M = EEM − stent) CSA, intrastent plaque (stent − lumen) CSA, arterial remodeling (ΔEEM CSA), tissue growth outside the stent (ΔP+M CSA) and tissue growth within the stent (Δstent − lumen CSA). Volumes were calculated using the Simpson rule.**

Results. **Mean EEM CSA increased significantly from 16.9 ± 5.0 mm^2 after intervention to 18.4 ± 4.9 mm^2 at follow-up ($p < 0.0001$), reflecting an increase in P+M CSA surrounding the stent (1.6 ± 1.3 mm^2). Greater tissue growth within the stent (2.4 ± 2.2 mm^2) correlated weakly, but directly with tissue growth surrounding the stent ($r = 0.356$, $p = 0.0121$). The ratio of peristent/intrastent tissue growth correlated weakly with arterial remodeling ($r = 0.282$, $p = 0.0525$). Restenotic stents had more tissue growth both within and surrounding the stent than did nonrestenotic stents. Volumetric measurements, which could be obtained in 15 lesions, showed similar results.**

Conclusions. **After implantation there is a chronic increase in plaque mass both within and surrounding the stents. The increase in peristent plaque mass is associated with adaptive remodeling.**

(J Am Coll Cardiol 1996;28:1134–9)

Intravascular ultrasound (IVUS) permits detailed, high quality, cross-sectional imaging of the coronary arteries in vivo. The normal coronary artery morphology (intima, media and adventitia), the major components of the atherosclerotic plaque (lipid, fibrous connective tissue and calcium), the intensely echoreflective (but relatively radiolucent) stainless-steel stent struts and the changes that occur in the atherosclerotic disease process, during transcatheter therapy, and in follow-up can be studied in vivo in a manner previously not possible using any other imaging modality.

From the Intravascular Ultrasound Imaging and Cardiac Catheterization Laboratories, Washington Hospital Center, Washington, D.C. This study was supported in part by the Cardiology Research Foundation, Washington, D.C. and the Heinrich-Hertz Stiftung, Dusseldorf, Germany. Dr. Leon is a consultant to Johnson & Johnson Interventional Systems, Warren, New Jersey.

Manuscript received March 13, 1996; revised manuscript received May 30, 1996, accepted June 11, 1996.

Address for correspondence: Dr. Martin B. Leon, Director of Research, Washington Cardiology Center, 110 Irving Street NW, Suite 4B1, Washington, D.C. 20010.

Recent IVUS studies have indicated that late lumen loss after interventional procedures in nonstented lesions is determined primarily by the direction and magnitude of arterial remodeling (1), not by cellular proliferation as was originally thought (2,3). An increase in arterial cross-sectional area (CSA) is adaptive; analogous to adaptive remodeling in early atherosclerosis, adaptive remodeling after catheter-based interventions results in a decreased incidence of restenosis despite an increase in plaque mass. In contrast, a decrease in arterial CSA leads to lumen compromise and restenosis.

In two randomized clinical trials Palmaz-Schatz tubular-slotted, stainless-steel stents reduced the rate of restenosis compared with balloon angioplasty (4,5), presumably by inhibiting acute elastic recoil and chronic pathologic arterial remodeling (6,7). Serial IVUS studies have shown 1) that tubular-slotted stents do not recoil over time; 2) that there is a stent-related increase in neointimal hyperplasia; and 3) that late lumen loss in stented lesions is almost completely the result of in-stent neointimal hyperplasia (8,9). However, it is not known whether tissue proliferation within the stents is

Published by Elsevier Science Inc.

0735-1097/96/$15.00
PII S0735-1097(96)00278-1

Abbreviations and Acronyms

CSA = cross-sectional area
EEM = external elastic membrane
IVUS = intravascular ultrasound
P+M = plaque plus media

associated with tissue proliferation surrounding the stents, and whether stents inhibit adaptive as well as pathologic remodeling.

The aim of this study was to assess the peristent chronic arterial responses to determine 1) whether tissue proliferation also occurs in native coronary arteries surrounding Palmaz-Schatz stents, and 2) whether tissue proliferation surrounding the stents is associated with adaptive arterial remodeling of the native vessel wall.

Methods

Patients and lesions. This study required adequate visualization of the deeper arterial structures surrounding the struts of the tubular-slotted, stainless-steel Palmaz-Schatz stents (Johnson & Johnson Interventional Systems). Although metal causes acoustic shadowing, Palmaz-Schatz stents cover only 10% to 15% of the endovascular surface; thus, there is adequate visualization of the deep wall structures in some but not all lesions. However, this is inconsistent and unpredictable; as a result, it was necessary to screen both postintervention and follow-up IVUS images in 81 stents from 61 lesions to identify a cohort with adequate visualization of the media-adventitia border for serial analysis. A study that was adequate for analysis had visualization of at least 80% of the circumference of the external elastic membrane (EEM) CSA over at least a 4-mm length of the stented segment in both the postintervention and follow-up studies.

We were able to analyze postintervention and follow-up IVUS studies in 49 stents from 39 native vessel lesions in 35 patients (29 men and 6 women, age 63 ± 11 years). At the time of stent implantation, 34% of the patients had a history of myocardial infarction, 17% presented with unstable angina and 60% presented with stable or progressive angina. At the time of follow-up, 9% of the patients had experienced a myocardial infarction, 14% presented with unstable angina and 57% presented with stable angina.

Twenty-nine lesions were treated with a single stent and 10 lesions were treated with two stents; three stents were articulated "biliary" stents (PS204), and 46 were coronary stents. Of the coronary stents, 20 were 3.0 mm, 20 were 3.5 mm and 6 were 4.0 mm in diameter. Stent location was the left anterior descending coronary artery in 15, the left circumflex artery in 8 and the right coronary artery in 26. The poststent implantation adjunct balloon size was 3.5 ± 0.4 mm, and the poststent implantation adjunct balloon inflation pressure was 16 ± 4 atm.

Intravascular ultrasound imaging protocol. The studies were performed using one of two commercially available systems. The first system (CVIS/InterTherapy Inc.) incorporated a single-element, 25-MHz transducer and an angled mirror mounted on the tip of a flexible shaft, which was rotated at 1,800 rpm within a 3.9F short monorail polyethylene imaging sheath to form planar cross-sectional images in real time. The second system (Cardiovascular Imaging Systems, Inc.) used a 30-MHz, single-element, beveled transducer mounted on the end of a flexible shaft and rotated at 1,800 rpm within either a 2.9F long monorail/common distal lumen imaging sheath or a 3.2F short monorail imaging sheath. With both systems, the transducer was withdrawn within the stationary imaging sheath at a speed of 0.5 mm/s using a motorized transducer pullback device. Motorized transducer pullback through a stationary imaging sheath permitted the transducer to move at the same speed as the proximal end of the catheter and facilitated comparative measurements on serial studies; this has been validated in vivo (10).

All IVUS studies were performed after administration of 0.2 mg of intracoronary nitroglycerin. To perform the imaging sequence the transducer was positioned approximately 10 mm beyond the distal edge of the stent and the motorized transducer pullback device was activated, and imaging continued until the transducer reached the aorto-ostial junction. Studies were recorded onto high resolution s-VHS videotape for off-line analysis. Patients were studied only after giving written, informed consent; all IVUS studies have the ongoing approval of the Washington Hospital Institutional Review Board.

Quantitative IVUS analysis. Using the motorized transducer pullback device, each stent was divided into 1-mm long axial segments. At a pullback speed of 0.5 mm/s, 1 mm of axial stent length equaled 2 s of videotape. In 15 of the stents, the EEM, stent and lumen CSAs could be measured in all image slices. In the remaining 34 stents, the EEM, stent and lumen CSAs could be measured in a variable number of contiguous images slices over at least a 4 mm of axial stent length.

Validation of cross-sectional measurements of EEM, stent, lumen and plaque plus media (P+M) CSAs by IVUS has been previously reported (11–15). The term *external elastic membrane* corresponds to the media-adventitia border, which is a reproducible measurement of the total arterial CSA. Because media thickness could not be measured accurately, P+M CSA was used as a measurement of the amount of atherosclerotic plaque. When the tissue encompassed the catheter, the lumen was assumed to be the size of the imaging catheter.

Using computerized planimetry, each border (EEM, stent and lumen) was routinely traced two to four times (Fig. 1). The following calculations were then made for each image slice. Finally, the results for each stent were averaged: 1) arterial remodeling (mm^2) = Δ (after intervention to follow-up) EEM CSA; 2) chronic stent recoil (mm^2) = Δ (after intervention to follow-up) stent CSA; 3) in-stent plaque CSA (mm^2) = stent CSA − lumen CSA; 4) peristent P+M CSA (mm^2) = EEM CSA − stent CSA; 5) in-stent tissue growth (mm^2) = Δ (after intervention to follow-up) intrastent plaque CSA; 6) peristent

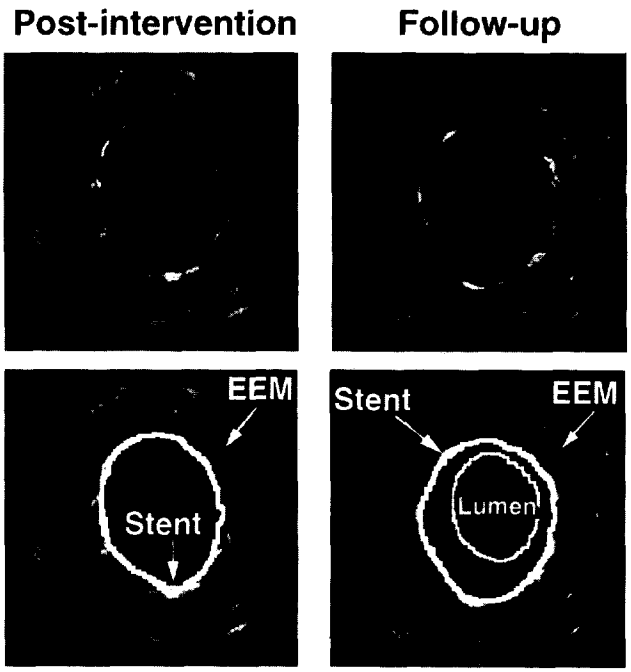

Figure 1. Planar intravascular ultrasound images of a Palmaz-Schatz stent after intervention and at follow-up are shown. Each is duplicated, and the duplicate is labeled. After intervention, the EEM CSA measured 17.9 mm^2, the stent CSA measured 8.4 mm^2, and the peristent P+M (EEM − stent) CSA measured 9.5 mm^2. At follow-up, the EEM CSA increased to 22.5 mm^2 (a 26% increase), the stent CSA did not change, and the lumen CSA decreased to 4.1 mm^2. Thus, there was 4.3 mm^2 of in-stent neointimal tissue proliferation (stent − lumen CSA) and an increase of 4.6 mm^2 (48%) in peristent P+M CSA.

tissue growth (mm^2) = Δ (after intervention to follow-up) peristent P+M CSA; and 7) total tissue growth (mm^2) = in-stent tissue growth + peristent tissue growth. *Arterial remodeling* was defined as adaptive (increase in EEM CSA) or pathologic (decrease in EEM CSA).

In the 15 stents with complete visualization of the EEM CSA, a similar serial analysis of the EEM, stent and lumen volumes was also performed. External elastic membrane, stent, lumen and plaque volumes (both within and surrounding the stent) were calculated using the Simpson rule. These methods have been reported previously (16,17).

The minimal lumen CSA within each stent was compared with the reference segment. The *reference segment* was defined as the most normal-looking cross section within 5 mm proximal and distal to the stented lesion, but before any major side branch. If a stent was placed in an ostial location, only a distal reference segment was measured. *Restenosis* was defined as ≥75% area stenosis when the minimal lumen CSA within the stent was compared with the reference lumen CSA (average of the proximal and distal reference lumen CSAs).

Reproducibility of IVUS measurements. The reproducibility of stent, lumen and EEM CSAs in our laboratory has been reported previously (1,18). However, because of the difficulty in visualizing the EEM through the stent struts, the reproducibility of the measurement was assessed specifically for the current study. In both postintervention and follow-up studies, the EEM CSA was measured twice in 10 stents. Repeated measurements were performed at least 2 months apart.

Table 1. Planar Intravascular Ultrasound Measurements of External Elastic Membrane, Stent and Lumen Cross-Sectional Areas After Intervention and at Follow-Up for All 49 Lesions

	After Intervention	Follow-Up	p Value
Mean EEM CSA (mm^2)	16.9 ± 5.0	18.4 ± 4.9	< 0.0001
Mean stent CSA (mm^2)	8.2 ± 2.4	8.2 ± 2.2	0.2127
Mean lumen CSA (mm^2)	8.2 ± 2.2	5.6 ± 2.2	< 0.0001
Mean intrastent plaque CSA (mm^2)	0.0 ± 0.1	2.4 ± 2.2	< 0.0001
Mean peristent plaque CSA (mm^2)	8.7 ± 3.3	10.4 ± 3.3	< 0.0001

Data presented are mean value ± SD. CSA = cross-sectional area; EEM = external elastic membrane.

Statistics. Statistical analysis was performed using StatView 4.02 (Abacus Concepts). Quantitative data were presented as mean value ± SD. Comparisons between groups were performed using paired and unpaired *t* tests for continuous variables or factorial analysis of variance (with post hoc analysis using the Fisher protected least significant difference), as appropriate. The level of significance was $p \leq 0.05$.

Results

Cross-sectional area measurements (Table 1). The postintervention reference lumen CSA measured 9.4 ± 3.7 mm^2.

Postintervention and follow-up EEM, stent and lumen CSAs could be evaluated in a total of 589 stent image slices within the 49 stents for a mean of 12 image slices per stent. Overall, the mean stent CSA did not change (8.2 ± 2.4 to 8.2 ± 2.2 mm^2, p = NS). The mean lumen CSA decreased from 8.2 ± 2.2 mm^2 after intervention to 5.6 ± 2.8 mm^2 at follow-up, entirely as a result of an increase in tissue within the stent. Similarly, the mean EEM CSA increased significantly from 16.9 ± 5.0 mm^2 after intervention to 18.4 ± 4.9 mm^2 at follow-up, as a result of a mean increase in P+M CSA surrounding the stent (from 8.7 ± 3.3 to 10.4 ± 3.3 mm^2, Fig. 1). The results are also shown in Figure 2.

Total mean tissue growth measured 4.1 ± 2.8 mm^2. Mean tissue growth within the stent was greater than mean tissue growth surrounding the stent (2.4 ± 2.2 vs. 1.6 ± 1.3 mm^2, p = 0.0015). The two were weakly but directly correlated (r = 0.356, p = 0.0121).

Arterial remodeling (Δ mean EEM CSA) correlated strongly with mean peristent tissue growth (r = 0.938, p < 0.0001) and moderately with mean total tissue growth (r = 0.628, p < 0.0001), but only weakly with mean in-stent tissue growth (r = 0.278, p = 0.0528).

Neither mean total tissue growth, mean peristent tissue growth, mean in-stent tissue growth, nor the ratio of mean in-stent/mean peristent tissue growth correlated with mean postintervention EEM, stent, lumen or peristent P+M CSAs.

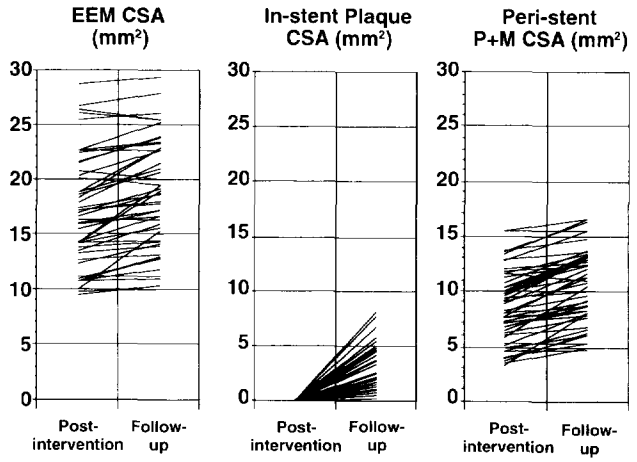

Figure 2. Planar IVUS results of the mean (per stent) postintervention and follow-up EEM, in-stent plaque and peristent P+M CSAs, in the total cohort of 49 stented lesions.

The ratio of mean peristent/mean instent tissue growth correlated weakly with arterial remodeling ($r = 0.282$, $p = 0.0525$). The mean peristent tissue proliferation tended to be inversely related to the mean postintervention peristent P+M CSA ($r = 0.220$, $p = 0.1295$).

There was no predilection for peristent tissue proliferation and adaptive remodeling to occur preferentially at any particular location within the stents (e.g., stent margins vs. stent bodies vs. central articulation).

The image slice with the smallest lumen CSA in each of the 49 stents was compared with the mean cross-sectional measurements. There was significantly more lumen loss (3.9 ± 2.2 vs. 2.6 ± 2.2 mm^2, $p < 0.0001$) and significantly more tissue growth within the stent (3.9 ± 2.2 vs. 2.4 ± 2.1 mm^2, $p < 0.0001$). The late increase in EEM area (1.8 ± 1.9 vs. 1.5 ± 2.0 mm^2, $p = 0.1162$) and the amount of peristent tissue proliferation (1.8 ± 1.8 vs. 1.6 ± 2.0 mm^2, $p = 0.3613$) were similar.

Restenotic versus nonrestenotic stents. Twenty-four stents were restenotic and 25 were nonrestenotic (Table 2). Restenotic stents tend to be smaller, have more in-stent and peristent tissue proliferation and have a greater late increase in EEM CSA.

Volumetric IVUS measurements (Table 3). Volumetric analysis was possible in seven restenotic and eight nonrestenotic stents. The postintervention and follow-up measurements in these 15 stents were similar to the 34 stents in which only limited analysis was possible.

Volumetric analysis paralleled the cross-sectional analysis. Overall, stent volume did not change (126 ± 36 to 123 ± 35 mm^3). Lumen volume decreased from 126 ± 36 mm^3 after intervention to 84 ± 49 mm^3 at follow-up, as a result of an increase of 37 ± 32 mm^3 in tissue volume within the stent. The EEM volume increased significantly from 246 ± 66 mm^3 after intervention to 263 ± 71 mm^3, as a result of an increase in tissue surrounding the stent (from 120 ± 45 to 138 ± 45 mm^3).

Table 2. Comparison of Serial Planar Intravascular Ultrasound Findings in Restenotic Versus Nonrestenotic Lesions

	Restenosis (n = 24)	No Restenosis (n = 25)	p Value
Mean postintervention EEM CSA (mm^2)	16.1 ± 4.0	17.7 ± 5.8	0.2476
Mean postintervention lumen CSA (mm^2)	7.6 ± 1.8	8.8 ± 2.4	0.0581
Mean postintervention peristent plaque CSA (mm^2)	8.4 ± 2.8	8.9 ± 3.7	0.6481
Mean follow-up lumen CSA (mm^2)	3.6 ± 1.9	7.5 ± 2.2	< 0.0001
ΔMean EEM CSA (mm^2)	1.9 ± 1.6	1.1 ± 1.3	0.0545
ΔMean stent CSA (mm^2)	0.0 ± 0.5	0.2 ± 0.5	0.3247
ΔMean lumen CSA (mm^2)	4.0 ± 2.3	1.3 ± 0.8	< 0.0001
ΔMean intrastent plaque CSA (mm^2)	4.0 ± 2.1	1.2 ± 0.7	< 0.0001
ΔMean peristent plaque CSA (mm^2)	1.9 ± 1.4	1.3 ± 1.0	0.0640
ΔMean total (intrastent + peristent) plaque CSA (mm^2)	5.9 ± 2.8	2.4 ± 1.5	< 0.0001

Data presented are mean value ± SD. Abbreviations as in Table 1.

Tissue growth within the stent (37 ± 32 mm^3) was greater than tissue growth surrounding the stent (19 ± 18 mm^3, $p = 0.0204$).

Reproducibility of EEM measurements. In 10 stented lesions repeated measurement of the EEM CSA was performed in 119 image slices after intervention and in 117 image slices at follow-up. The difference in repeated measurements of the postintervention EEM CSA was 4.0 ± 2.9%; the difference in repeated measurements of the follow-up EEM CSA was 4.3 ± 3.6%. Correlation of repeated measurements for all 236 image slices was $r = 0.96$.

Discussion

This study shows that endovascular tubular-slotted, stainless-steel stents induce tissue proliferation both within the endoluminal stent surface and in the tissue layers surrounding the metallic Palmaz-Schatz stent struts. Both in-stent and peristent tissue proliferation is greater in restenotic than in nonrestenotic stents. Tissue proliferation surrounding the Palmaz-Schatz stents is accompanied by adaptive remodeling (increase in EEM CSA).

Table 3. Intravascular Ultrasound Measurements of External Elastic Membrane, Stent and Lumen Volumes After Intervention and at Follow-Up for 15 Lesions Suitable for Volumetric Analysis

	After Intervention	Follow-Up	p Value
EEM volume (mm^3)	246 ± 66	263 ± 71	0.0067
Stent volume (mm^3)	126 ± 36	123 ± 35	0.9821
Lumen volume (mm^3)	126 ± 36	84 ± 49	0.0013
Intrastent plaque volume (mm^3)	0 ± 0	37 ± 32	< 0.0001
Peristent plaque volume (mm^3)	120 ± 45	138 ± 45	0.0039

Data presented are mean value ± SD. EEM = external elastic membrane.

Tissue proliferation after stent placement. Previous studies have indicated that intraluminal tissue proliferation within tubular-slotted stents is a complex process involving an early thrombotic layer, which, over a period of weeks, is replaced by fibromuscular cells, extracellular matrix and eventually collagen (19–21). In animal models, maximal neointimal thickness occurs at approximately 8 weeks after stent implantation; this is followed by scarring and thinning (19).

The current IVUS study suggests that this process may also occur in the tissue layers surrounding the stents. As with in-stent neointimal tissue proliferation, which has been shown to be uniformly distributed over the length of the stent (9), there was no predilection for peristent tissue proliferation to be located at the ends, bodies or central articulation of the Palmaz-Schatz stent.

There was a direct but weak correlation between the increase in plaque mass inside and outside of the stent. There are several possible explanations for this weak correlation. Neointimal tissue proliferation inside the stent and the increase in P+M outside the stent may, in part, have different mechanisms. In-stent neointimal tissue proliferation may be a homogeneous process, whereas the peristent increases in plaque mass may represent the net result of smooth muscle cell proliferation and either growth or apoptosis of the existing atherosclerotic plaque. Early platelet activation or thrombus formation, or both, on the inner surface of the stent (which may not occur on the outer surface of the stent, where there is stent-tissue contact) may lead to preferential endoluminal tissue proliferation. There may be variations in smooth muscle cell migration, as well as different degrees of smooth muscle cell proliferation, in media versus neointima. Alternatively, the variation in the remodeling responses of the deep wall structures may contribute to the relative amounts in-stent versus peristent tissue accumulation. Greater adaptive remodeling (increase in EEM CSA) may facilitate peristent tissue accumulation, although deep wall structures that are resistant to adaptation may force tissue proliferation to be confined to the endoluminal surface of the stent. In the current study there was a weak correlation between the ratio of peristent/in-stent tissue accumulation and the degree of adaptive arterial remodeling.

Arterial remodeling after stent placement. Stents cause several changes in the surrounding media and adventitia. Short-term effects of stent placement on the vessel wall include thinning of the media and possible rupture of the internal elastic membrane (22), whereas long-term include inflammatory infiltrates surrounding the stent wires, replacement of the media by myofibroblastic proliferation and increases in the collagen and mucopolysaccharide content of the media (22). Although these changes may otherwise lead to pathologic remodeling (decrease in external EEM CSA) and restenosis (as occurs in nonstented lesions), stents have been shown to reduce restenosis, in part, by virtually eliminating pathologic arterial remodeling.

The Serial Ultrasound Analysis of Restenosis (SURE) trial has demonstrated that remodeling after nonstent interventions is biphasic with early adaptive remodeling (increase in external EEM CSA at 1 month) and late pathologic remodeling (decrease in EEM CSA at 6 months) (23). When it is sustained, adaptive remodeling has been shown to accommodate neointimal tissue growth to prevent restenosis in both animal models and humans (1,24). This may be analogous to arterial remodeling in the early atherosclerotic disease process, in which plaque accumulation is compensated for by an increase of total vessel CSA, and lumen compromise is delayed until plaque accumulation outstrips the adaptive capacities of the artery (25–27). Although stents prevent late pathologic remodeling, the current study shows that stents do not inhibit early adaptive arterial remodeling. In some lesions this may represent an additional means of accommodating the stent-related neointimal tissue proliferation. However, whether or not stents limit the magnitude of the potential adaptive remodeling responses in the instrumented artery cannot be determined from the current study.

Study limitations. This study represented a selected series of lesions studied after intervention and at follow-up. There may have been a selection bias 1) because of the nature of the follow-up, and 2) because less than 50% of the stented lesions for which we had serial IVUS studies were adequate for serial analysis of the peristent vascular changes. The ability to visualize the deep arterial structures through the stent struts was unpredictable. Furthermore, because the analysis was limited to image slices in which the EEM could be well visualized through the stent struts, it was not possible to relate peristent arterial responses to the original lesion (either the location of the center of the lesion or the underlying plaque composition). However, this was intended as a mechanistic study, and was not designed to determine the predictors of these peristent vascular responses. Finally, whether these findings apply to other stents, as well, cannot be determined from this study.

Conclusions. In-stent restenosis is the result of endovascular neointimal tissue proliferation, accompanied by a lesser amount of peristent tissue proliferation. Palmaz-Schatz stents prevent pathologic remodeling but not adaptive remodeling. Adaptive remodeling surrounding Palmaz-Schatz stents presumably occurs in response to peristent tissue proliferation. The ultimate effect of these peristent arterial responses is unknown.

References

1. Mintz GS, Popma JJ, Pichard AD, et al. Arterial remodeling after coronary angioplasty: a serial intravascular ultrasound study. Circulation. 1996;94:35–43.
2. Austin GE, Ratliff NB, Hollman J, Tabei S, Phillips DF. Intimal proliferation of smooth muscle cells as an explanation for recurrent coronary artery stenosis after percutaneous transluminal coronary angioplasty. J Am Coll Cardiol 1985;6:369–75.
3. Clowes AW, Schwartz SM. Significance of quiescent smooth muscle migration in the injured rat carotid artery. Circ Res 1985;56:139–45.
4. Fischman DL, Leon MD, Baim DS, et al. A randomized comparison of coronary-stent placement and balloon angioplasty in treatment of coronary artery disease. N Engl J Med 1994;331:496–501.
5. Serruys PW, de Jaeger P, Kiemeneij F, et al. A comparison of balloon-

expandable-stent implantation with balloon angioplasty in patients with coronary heart disease. N Engl J Med 1994;331:489–95.

6. Mintz GS, Pichard AD, Kent KM, et al. Endovascular stents reduce restenosis by eliminating geometric arterial remodeling: a serial intravascular ultrasound study [abstract]. J Am Coll Cardiol 1995;25:36A.
7. Gordon PC, Gibson CM, Cohen DJ, Carrozza JP, Kuntz RE, Baim DS. Mechanism of restenosis and redilatation within coronary stents: quantitative angiographic assessment. J Am Coll Cardiol 1993;21:1166–74.
8. Painter JA, Mintz GS, Wong SC, et al. Serial intravascular ultrasound studies fail to show evidence of chronic Palmaz-Schatz stent recoil. Am J Cardiol 1995;75:398–400.
9. Hoffmann R, Mintz GS, Popma JJ, et al. Distribution of tissue growth in Palmaz-Schatz stents: insights from a serial intravascular ultrasound study [abstract]. J Am Coll Cardiol 1996;27:138A.
10. Fuessl RT, Mintz GS, Pichard AD, et al. In vivo validation of intravascular ultrasound length measurements using a motorized transducer pullback device. Am J Cardiol 1996;77:1115–8.
11. Nishimura RA, Edwards WD, Warnes CA, et al. Intravascular ultrasound imaging: in vitro validation and pathologic correlation. J Am Coll Cardiol 1990;16:145–54.
12. Tobis JM, Mallery J, Mahon D, et al. Intravascular ultrasound imaging of human coronary arteries: in vivo analysis of tissue characterization with comparison to in vitro histological specimens. Circulation 1991;83:913–26.
13. Gussenhoven EJ, Essed CE, Lancee CT, et al. Arterial wall characteristics determined by intravascular ultrasound imaging: an in vitro study. J Am Coll Cardiol 1989;14:947–52.
14. Nissen SE, Grines CL, Gurley JC, et al. Application of a new phased-array ultrasound imaging catheter in the assessment of vascular dimensions: in vivo comparison to cineangiography. Circulation 1990;81:660–6.
15. Potkin BN, Bartorelli AL, Gessert JM, et al. Coronary artery imaging with intravascular high-frequency ultrasound. Circulation 1990;81:1575–85.
16. Matar FA, Mintz GS, Farb A, et al. The contribution of tissue removal to lumen improvement after directional coronary atherectomy. Am J Cardiol 1994;74:647–50.
17. Dussaillant GR, Mintz GS, Pichard AD, et al. Small stent size and intimal hyperplasia contribute to restenosis: a volumetric intravascular ultrasound analysis. J Am Coll Cardiol 1995;26:720–4.
18. Mintz GS, Griffin J, Chuang YC, et al. Reproducibility of the intravascular ultrasound assessment of stent implantation in saphenous vein grafts. Am J Cardiol 1995;75:1267–70.
19. Schatz RA, Palmaz JC, Tio FO, Garcia FJ, Reuter SR. Balloon-expandable intracoronary stents in the adult dog. Circulation 1987;76:450–7.
20. van Beusekom HMM, van der Giessen WJ, van Suylen RJ, Bos E, Bosman FT, Serruys PW. Histology after stenting of human saphenous vein bypass grafts: observations from surgically excised grafts 3 to 320 days after stent implantation. J Am Coll Cardiol 1993;21:45–54.
21. Palmaz JC. Intravascular stents: tissue-stent interactions and design considerations. Am J Roentgenol 1993;160:613–8.
22. Karas SP, Gravanis MB, Santoian EC, Robinson KA, Anderberg KA, King SB III. Coronary intimal proliferation after balloon injury and stenting in swine: an animal model of restenosis. J Am Coll Cardiol 1992;20:467–74.
23. Kimura T, Kaburagi S, Tashima Y, Nobuyoshi M, Mintz GS, Popma JJ. Geometric remodeling and intimal regrowth as mechanisms of restenosis: observations from Serial Ultrasound Analysis of Restenosis (SURE) trial [abstract]. Circulation 1995;92 Suppl I:I-76.
24. Kakuta T, Currier JW, Haudenschild CC, Ryan TJ, Faxon DP. Differences in compensatory vessel enlargement, not intimal formation, account for restenosis after angioplasty in the hypercholesterolemic rabbit model. Circulation 1994;89:2809–15.
25. Stiel GM, Stiel LG, Schofer J, Donath K, Mathey DG. Impact of compensatory enlargement of atherosclerotic coronary arteries on angiographic assessment of coronary disease. Circulation 1989;80:1603–9.
26. Glagov S, Weisenberg E, Zarins CK, Stankunacicius K, Kolettis GJ. Compensatory enlargement of various human atherosclerotic arteries. N Engl J Med 1987;316:1371–5.
27. McPherson DD, Sirna SJ, Hiratzka LF, et al. Coronary arterial remodeling studied by high-frequency epicardial echocardiography: an early compensatory mechanism in patients with obstructive coronary atherosclerosis. J Am Coll Cardiol 1991;17:79–86.